Available online at www.sciencedirect.com
ScienceDirect
Ceramics International 37 (2011) 759–769
CERAMICS INTERNATIONAL
www.elsevier.com/locate/ceramint

# Studies on novel bioactive glasses and bioactive glass–nano-HAp composites suitable for coating on metallic implants

Chidambaram Soundrapandian, Sanghamitra Bharati, Debabrata Basu, Someswar Datta *

*Bioceramics & Coating Division, Central Glass & Ceramic Research Institute, Kolkata 700032, India*

Received 24 February 2010; received in revised form 24 June 2010; accepted 6 October 2010
Available online 23 November 2010

**Abstract**

A series of novel zinc oxide (ZnO) containing bioactive glass compositions in $SiO_2$–$Na_2O$–CaO–$P_2O_5$ system and composite with hydroxyapatite (HAp) nano-particles were developed and applied as coating on Ti–6Al–4V substrates. The bioactive glasses and their composites were also processed to yield dense scaffolds, porous scaffolds and porous bone filler materials. The coating materials and the coatings were characterized and evaluated by different in vitro techniques to establish their superior mechanical properties. The cytotoxicity test of the coating material, porous and dense scaffolds and coated specimens showed non-cytotoxicity, biocompatibility and promising in vitro bioactivity for all tested samples. The dissolution behaviour studies of the bioactive glasses and the composites in simulated body fluid showed promising in vitro release pattern and bioactivity for all tested samples. Addition of nanosized HAp improves mechanical properties of the bioactive glass coating without affecting the in vitro bioactivity.


*Keywords:* B. Nanocomposites; D. Glass ceramics; D. Apatite; E. Biomedical applications

## 1. Introduction

Metallic load bearing implants are often coated with other bioactive materials such as hydroxyapatite (HAp), bioactive glass and others by various techniques to improve their surface bioactivity, adherence to the adjacent hard tissues and to enable cementless fixation [1–5]. The first attempt of Tomsia et al. [3,4] to develop bioactive glass coated implants of titanium alloys possess serious drawback of thermal expansion mismatch between the glass and the substrate; which on heat treatment resulted with interfacial cracks that propagated eventually leading to delamination of the coating. Moreover, bioactive glasses are normally very brittle and prone to crack propagation leading to catastrophic failure.

Recent literature shows that release of small concentration of zinc (Zn) from an implant material could promote bone formation around the implant and accelerate recovery of the patients [6–10]. Materials containing Zn promote the expression and maintenance of the osteoblastic phenotype, and Zn present at resorptive sites is connected with the recruitment of osteoblastic cells and bone renewal [11,12]. Moreover, Zn is well known for its antimicrobial properties, and a constituent of the denture adhesive as a cross-linking agent to promote adhesion [13]. However, it is also important to control Zn releasing rate from the compositions, in order to prevent adverse reactions and to reduce glass degradation without affecting HA deposition. However, it is surprising that till date research on zinc containing bioactive glass is rather limited [14–17] and no report on coating of such glasses on load bearing metallic implant surfaces exist; where the impact would be maximum.

Our recent studies showed excellent bioactivity of some novel bioactive glasses containing $B_2O_3$ and $TiO_2$ [18–21]. The mechanical properties, particularly the scratch resistance property of the bioactive glassy and composite coating improved due to addition of nano hydroxyapatite crystals and by gamma sterilization [20]. In the present study, a series of suitable ZnO containing bioactive glasses synthesized by conventional melting technique have been formulated to coat on metallic implants. The glasses were characterized and used to coat Ti–6Al–4V alloy which is especially appropriate for

* Corresponding author. Tel.: +91 33 2473 3496/3469/3476/3477x3232; fax: +91 33 2473 0957.
*E-mail address:* sdatta@cgcri.res.in (S. Datta).

0272-8842/$36.00 
doi:10.1016/j.ceramint.2010.10.025

load bearing implants functioning under high stress, like hip, dental and artificial knee. The bioactive glass composite coatings with nano-HAp were developed to enhance coating adhesion and improve scratch resistance property. The thermal behaviour of the bioactive glass and composite materials were studied using differential thermal analysis, derivative differential thermal analysis, thermo gravimetric analysis and dilatometric studies. The dissolution test in simulated body fluid (SBF) [22] and distilled water were used to assay their ion release properties and cytotoxicity test used to evaluate the safety for biological behaviour.

## 2. Materials and methods

### 2.1. Preparation of bioactive-glass powder and bioactive glass coating on Ti6Al4V with and without nano-sized HAp powder

A series of glasses in the $SiO_2$–$Na_2O$–ZnO–CaO–MgO–$P_2O_5$ system (termed as BGZ series) were prepared from reagent grade quartz ($SiO_2$), calcium carbonate ($CaCO_3$), light magnesium carbonate ($MgCO_3$), dry soda ash ($Na_2CO_3$), di-ammonium hydrogen phosphate [$(NH_4)_2{\cdot}HPO_4$] and other minor ingredients using a conventional glass melting procedure. The oxide compositions of the glass system are shown in Table 1. The bulk glass was prepared by easy casting in preheated cast iron moulds followed by immediate annealing at 500 °C (close to the glass transition temperature) for 30 min followed by slow cooling. Bioactive glass–nano-HAp composites were prepared with nano-HAp constituting 10 or 25% the composition. The processing details for preparation of bioactive glass and the composite coating materials and coating on Ti–6Al–4V substrates were similar to our previous papers [18–21]. Similarly, the processing details for preparation of bioactive glass and the composite scaffolds were similar to our previous papers [18–21,23]. However, in case of composite scaffolds, the constituents including the pore former (β-napthalene) were mixed homogeneously before cold isostatic pressing. Porous bone filler materials were prepared by controlled grinding and sieving of porous scaffolds. Preparation and characterization details of nano-sized hydroxyapatite material used for this work were reported earlier [24].

Table 1
Oxide composition of different ZnO containing bio-glasses (mol.%).

| Components | BGZ-1 | BGZ-2 | BGZ-3 |
|---|---|---|---|
| $SiO_2$ | 55.90 | 58.0 | 61.24 |
| $Na_2O$ | 11.80 | 12.0 | 6.77 |
| $K_2O$ | 2.50 | – | 2.24 |
| CaO | 16.14 | 18.0 | 16.89 |
| MgO | 9.93 | 7.0 | 7.27 |
| ZnO | 1.24 | 2.4 | 2.24 |
| $P_2O_5$ | 2.50 | 2.6 | 3.35 |
| $\alpha$ (RT to 600 °C) | $128.1 \times 10^{-7}$ | $126.0 \times 10^{-7}$ | $110 \times 10^{-7}$ |
| Enamelling temperature | 800–820 °C | 800–820 °C | 800–820 °C |

### 2.2. Structural characterization

The thermal properties, differential thermal analysis (DTA), derivative differential thermal analysis (DDTA) and thermo gravimetric analysis (TGA) of the resultant glassy materials were studied by DTA/TGA (Netzsch, Germany). The measurements were conducted in ambient atmosphere, up to 900 °C, using a range of heating rates between 5 °C/min and 30 °C/min. Pure calcined α-alumina powder was used as reference material. The thermal expansions of the glasses were measured using an Orton Dilatometer-1600 D from room temperature to 600 °C.

XRD patterns of the glass powders and coatings were recorded on a Philips (Philips Analytical, X'Pert, 1830, Netherlands) diffractometer in the $2\theta$ range 20–70° using Cu $K_\alpha$ ($\lambda$ = 1.54056 nm) radiation for confirmation of the phases.

Microstructure of the coating surfaces and polished cross sections were studied using a SEM (LEO 430i, UK) along with EDX analysis using Si–Li detector to identify different area and phases in the microstructure.

Adhesion of the coating was estimated by scratch testing of the coating using a Ducom Scratch Tester TR-01 attached with a load cell of 200 N and using a Rockwell diamond indenter, while optical micrographs of the scratches were taken using an image analyzer (Correct, Seiwa Optical, Tokyo) for exact determination of the breaking load corresponding to the failure of the coating. A set of three coated samples were tested. On each sample two or more scratch marks studied to obtain the value of breaking load and the averages reported. The impact strength of the bioactive glass coating was tested by ''falling ball'' method using a 1.0 kg ball with 10 cm dia. head according to the IS: 3149-1994 specification.

The adhesion strength of the coatings was further measured by stud pull method using Romulus Universal Tester, an adhesion strength tester instrument (Quad Group Inc., Model No. Romulus, USA). As before, a set of three coated samples were tested to obtain average adhesion strength. Care was taken to ensure almost identical pull off in each case of measurement.

The Young's modulus, Vicker's hardness and fracture toughness of different bioactive glass coatings were determined by Instron machine and depth sensitive indentation technique (Fischerscope H100C $XY_p$, Fischer, Switzerland).

### 2.3. In vitro bioactivity evaluation of bioactive glass and coatings

#### 2.3.1. Dissolution studies of bioactive glass and bioactive glass coated Ti–6Al–4V samples

The dissolution study for different bioactive glass samples were carried out in simulated body fluid medium (SBF, pH 7.25) at 37 °C in an incubator to assess their acellular bioactivity. For $Zn^{++}$ release study similar conditions were maintained, but with double distilled water as the medium. The samples (pellets of 10 mm Φ and 3 mm thickness) were weighed to the accuracy of ±0.1 mg and placed in 25 ml SBF medium in an incubator for a predetermined period of time (1 week to 4 week). After required soaking period the solution was

removed for ion release ($Ca^{++}$ and $PO_4^{3-}$) analysis. Inductively coupled plasma atomic emission spectroscopy (ICP) analysis was conducted on the leached solutions resulting after dissolution of glass pellets using ICP analyzer (CIROS Vision FVS12, Spectro Analytical Instruments). The bioactive glass pellet after dissolution was first removed, the surface rinsed gently with distilled water and dried thoroughly. The microstructure was characterized by scanning electron microscope and the deposited phases were studied by EDX analysis to analyze the HAp forming ability of the glass surface.

#### 2.3.2. Cytotoxic evaluation of bioactive glass coated Ti–6Al–4V samples

The in vitro cytotoxicity test of bioactive glass powders, coatings on Ti–6Al–4V substrates, porous scaffolds and dense scaffolds were conducted to study their suitability for biomedical applications. The in vitro cytotoxicity test using direct contact method and test on extract method were performed using test samples, negative controls and positive controls. In direct method, all the specimens including negative control (ultra high molecular weight polyethylene) and positive control (PVC) were taken in triplicate and placed on subconfluent monolayer of L-929 mouse fibroblast cells using modified Eagle's medium (MEM) supplemented with foetal bovine serum as the culture medium. After incubation of cells with test samples at 37 ± 2 °C for 24 ± 1 h, cell culture was examined microscopically for cellular response around test samples.

In test on extract method, the extract was prepared by incubating test materials with physiological saline at 37 ± 2 °C for 72 ± 2 h and made up with medium to get an extraction ratio of 1.25 $cm^2$/ml. 100% extracts were diluted to get concentrations of 50% and 25% with media. Different dilutions of extracts of test samples, negative controls (ultra high molecular weight polyethylene) and positive controls (dilute phenol) in triplicate were placed on subconfluent monolayer of L-929 mouse fibroblast cells. After incubation of cells with extracts of test samples and controls at 37 ± 2 °C for 24 ± 1 h, cell culture was examined microscopically using a phase contrast microscope for cellular response.

## 3. Results and discussion

Bioactive glasses in $SiO_2$–$Na_2O$–CaO–$P_2O_5$ system [25] have higher bioactivity in comparison to hydroxyapatite and hence are a better choice for coating on metallic implants used in orthopaedic, dental and plastic surgery. The basic requirements for a bioactive glass to serve as a coating on different load bearing metallic implants (titanium and its alloy) are matching (preferably lower) thermal expansion coefficient (9.5–10.5 × $10^{-6}$/°C at RT to 400 °C). Further, to apply the coating by conventional vitreous enamelling technique the coating material should possess a softening temperature below the $\alpha \rightarrow \beta$ transition temperature (955–1010 °C) of titanium [26]. The glass compositions were formulated from $M_2O$–RO–ZnO–$SiO_2$ glass system, where M = Na, and K and R = Ca and Mg. The glass compositions (Table 1) were formulated with minor amount of ZnO and $P_2O_5$ addition in such a way that the thermal expansion coefficient ($\alpha$) matched with that of the substrate (Ti–6Al–4V alloy), exhibited low fusion temperature (to prevent excessive chemical reaction of titanium with molten glassy coating during coating fusion), release $Zn^{++}$ ion in a controlled way and bioactivity retained. The thermal analysis and dilatometric analysis results are shown in Table 1.

Nanosized HAp, the main inorganic constituent of human bone, synthesized in our lab (grain size ~100–250 μm and crystallite size in the range of 20–60 nm) was added to the bioactive glass to improve the bioactivity and scratch resistance of the composite coating. When dispersed in glass matrix, it formed a glass–ceramic that improved the mechanical properties of the composite coating. Since the mechanical properties of the glass–ceramic materials is strongly dependent on particle size of the crystallites and increases with decreasing particle size [27–29], nanosized HAp powder was used. In order to achieve a homogeneous microstructure in the resultant glass ceramic composite very fine glass particles (5–20 μm) are mixed thoroughly with HAp particles by milling in a planetary ball mill and applied as a coating by spraying or dipping.

### 3.1. Structural characterization

From DTA and DDTA results, glass softening temperature was found to be favourably <750 °C, preventing excessive oxidation of the substrate alloy while coating with bioactive glass or composite by vitreous enamelling technique. The linear coefficient of thermal expansion ($\alpha$) of the glasses were measured to be in the range of 11.0–12.8 × $10^{-6}$/°C at RT to 600 °C, which although in higher side, is comparable with that of the base metal.

The XRD analysis (Fig. 1) showed all the glass powders to be amorphous in nature, and the resultant coatings mainly amorphous in nature (presence of broad hump around 20–35°); with little volume fraction of crystalline phases ($Na_2Ca_2Si_3O_9$) (JCPDS – 22-1455) (Fig. 2).

#### 3.1.1. FTIR analysis

All the glasses exhibit similar FTIR spectra. The FTIR spectra (Fig. 3) show two broad strong absorption bands at ~1050 $cm^{-1}$ and 480 $cm^{-1}$ which can be assigned to Si–O and P–O vibrations, respectively. There are a number of small and broad bands at 570 $cm^{-1}$, which may be due to $PO_4^{3-}$ tetrahedral. The broad

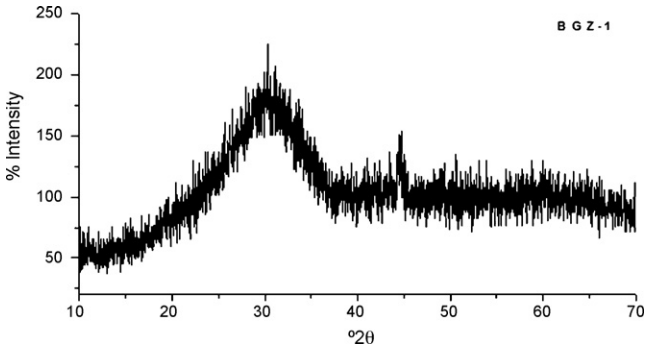


Fig. 1. Typical XRD pattern of bioactive glass powder.

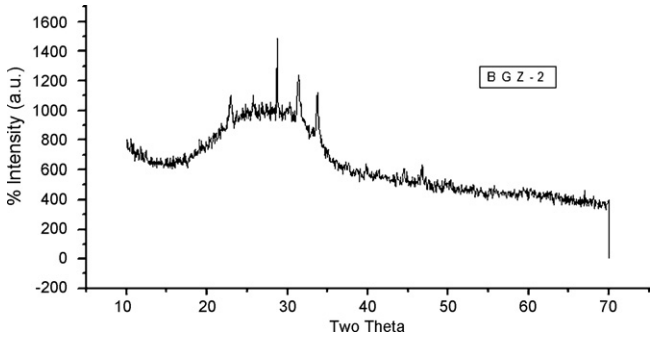


Fig. 2. XRD pattern of BGZ-2 coating.

small band at ~780 $cm^{-1}$ may be due to bending vibrations of Si–O–Si bridges [30]. However, the existence of different groups like Zn–O and phosphates cannot be pin pointed accurately because of super impositions of different peaks.

### 3.1.2. Mechanical properties

Mechanical properties of the glass coatings are presented in Table 2. The hardness and the Young's modulus values are superior compared to other bioactive glass coating compositions already reported by other researchers [31].

### 3.1.3. Thermal properties

The DTA patterns of these glasses change with heating rates. DTA curves of BGZ-1 powdered samples at different heating rates in the range of 5–30 °C/min are presented in Fig. 4. Although, the peak crystallization temperature was not very prominent indicating a predominantly stable glassy nature, the little exothermic hump shifted to a higher value with increase in rate of heating [600 °C at 30 °C/min heating rate to 540 °C at 5 °C/min heating rate], as reported in the literature [32]. The corresponding DDTA curves supported this observation. The TGA curves (Fig. 5), however, do not change significantly with heating rates. The absence of any definite nucleation and growth temperature over a wide range of heating rates is particularly important when application as scaffold or bone filler material is concerned, as the required microstructure and porosity in the product will remain unaffected by minor changes in the processing variables during fabrication.

A typical DTA/DDTA curve of one glass (BGZ-1) is shown in Fig. 6. BGZ-2 glass exhibited low maturing temperature

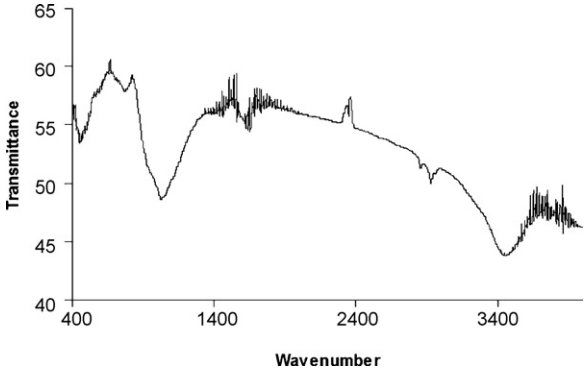


Fig. 3. A typical FTIR spectra of BGZ glasses.

Table 2
Mechanical properties of different bioactive glass.

| Glass code | Load (kg) | Young's modulus (GPa) | Vicker's hardness (GPa) | Fracture toughness (MPa $m^{1/2}$) |
|---|---|---|---|---|
| BAG | 1.0 | 72.0 | 6.52 | 0.74 |
| BGZ-1 | 1.0 | 72.0 | 9.39 | 0.62 |
| BGZ-2 | 1.0 | 72.0 | 11.59 | 0.53 |

compared to other glass. Fig. 7 shows linear change of length of different bioactive glasses with temperature, BAG-1 (a different bioactive glass reported earlier [18], green curve) is presented in Fig. 1 for ready comparison. The linear expansions of all the glasses were almost similar up to 400 °C and suitable for coating on Ti–6Al–4V substrate. The decrease in percent linear change (PLC) value in case of BGZ-1 after 525 °C is due to its lower softening point and hence the reading was taken up to 500 °C.

The thermal analysis results confirm that the Zn containing glasses are suitable for application as a coating on Ti–6Al–4V alloy substrates. The coating also retains its predominant glassy structure even when subjected to different heating rates. The glasses are relatively insensitive to minor change in thermal conditions.

### 3.1.4. Microscopic characterization

A typical SEM micrograph (Fig. 8) of the polished cross section of a bioactive glass coating (BGZ-2) showed existence of a clear interface between metal and coating. The interface is well diffused (20–40 μ) in metal side and coating indicating strong chemical bonding [33]. The EDX analysis (Fig. 9) around the interface line confirmed this observation with gradual change in concentration of Ti, Al and V indicating presence of metallic phase and Si, Na, Ca and Zn confirming simultaneous presence of glassy phase. The EDX analysis also confirmed the presence of Zn in the coating, though very minimum. The occasional presence of fine crystalline phases could be easily seen in the magnified view of the cross section of the bioactive coating surface presented in Fig. 10. This micrograph displays considerable amount of glassy phase present in the surface. The crystals are needle shaped and microcrystalline (<3.0 μm) in nature.

### 3.1.5. Scratch testing analysis of coatings

Scratch testing analysis of the coated samples were carried out to study the possible effects of surrounding hard tissues on the surface of the coated implants during primary insertion in the hard tissue of human body [18,34–36]. For cement less fixation of the load bearing orthopaedic or dental implants primary stability after fixation of the implant is mainly achieved by mechanical anchoring. As a result, considerable friction and abrasion occurs between the implant surface and the surrounding bones; which is best simulated using scratch testing equipment.

In case of hard and brittle bioactive glass or composite coating on ductile metallic substrate of Ti6Al4V alloy, three

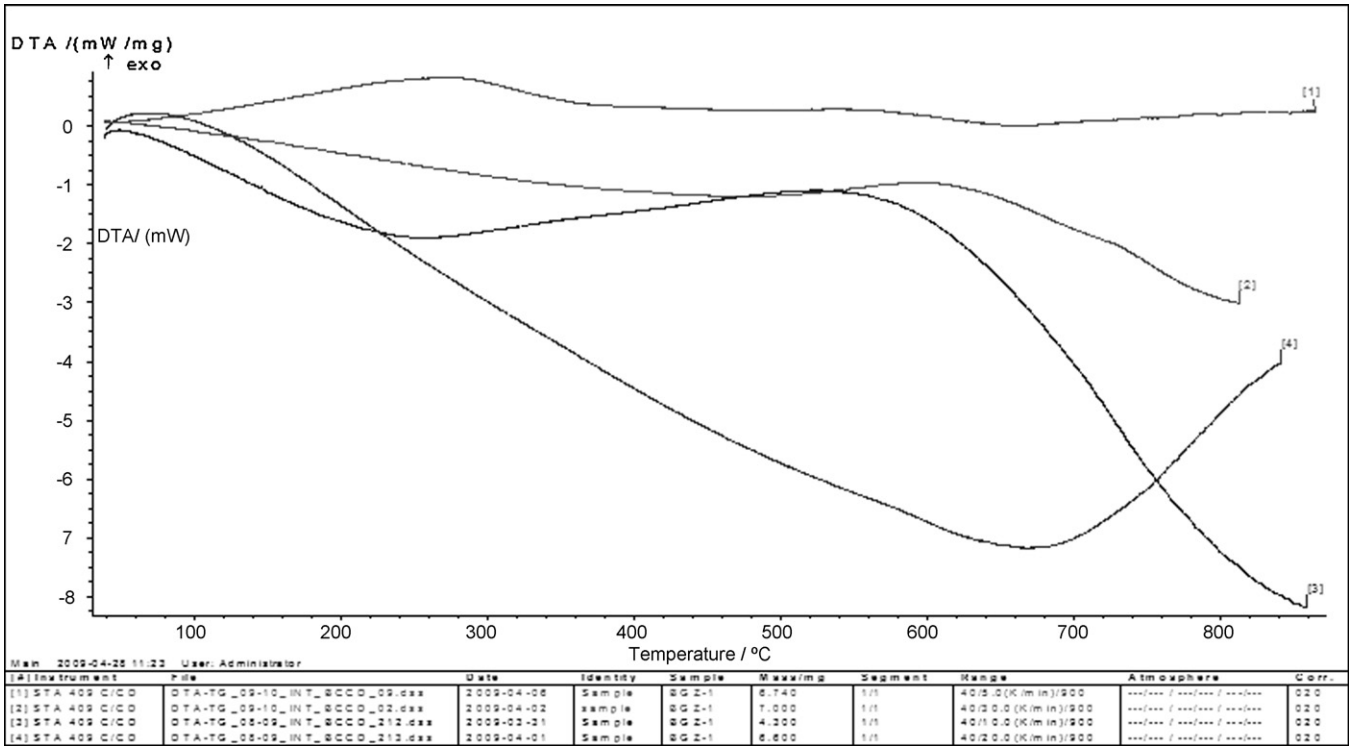


Fig. 4. DTA plots of BGZ-1 at different heating rates.

different types of failure mode can operate simultaneously, (i) through-thickness cracking, (ii) coating detachment and (iii) chipping within the coating. Examination of optical micrographs of scratch tested samples (Figs. 11–14) reveals that all of them are operating simultaneously with varying intensity depending upon the nature of the coating. In case of glassy coatings without any second phase addition, effect of (ii) and (iii) was prominent but in case of composite coating the scratch pattern became smooth and effect of all the mechanisms were less prominent.

From the results shown in Table 3, it was observed that the breaking load (adhesion strength) were lower for only glassy

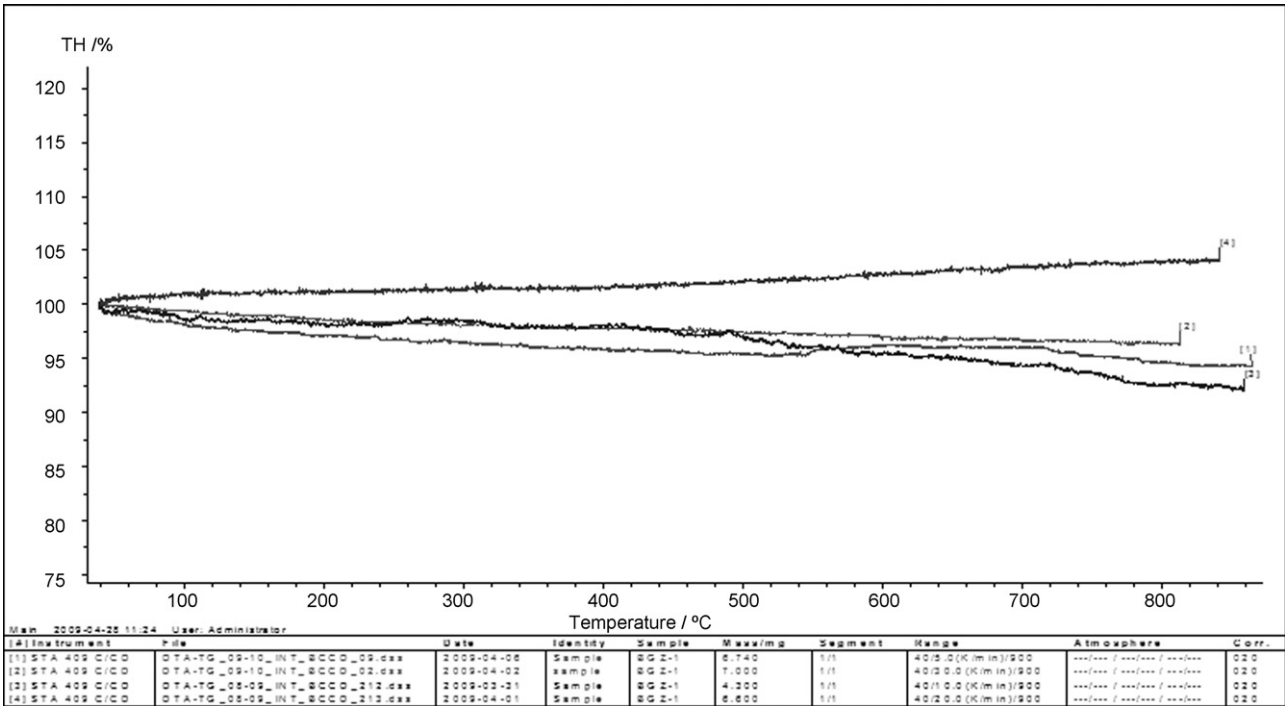


Fig. 5. TGA plots of BGZ-1 at different heating rates.

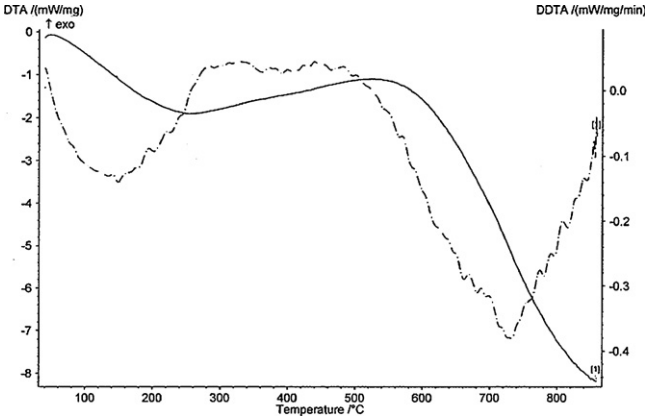


Fig. 6. DTA and DDTA curve for BGZ-1 at heating rate of 10 °C/min.

coatings (21N and 41.5N for BGZ-1 and BGZ-2 respectively) than that of nano-HAp composite (10 wt%) glass ceramic coating (26.5N and 42.5N for BGZ-1 and BGZ-2 composite

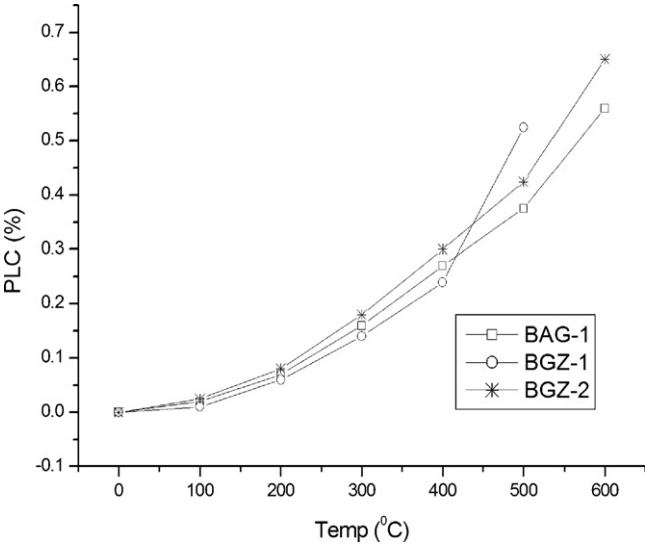


Fig. 7. % Linear change of length of different bioactive glasses with temperature.

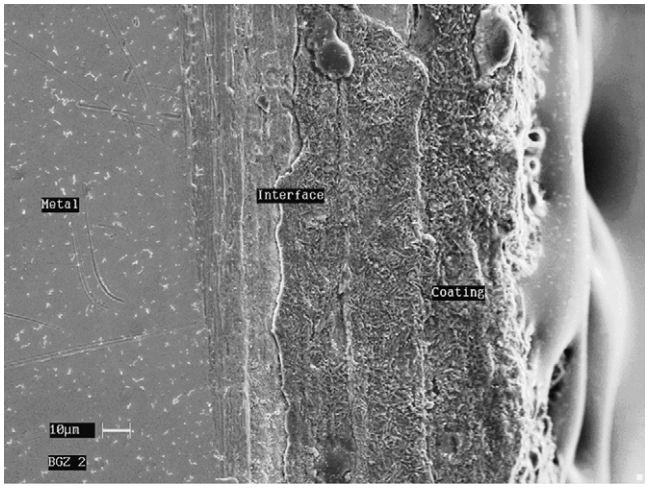


Fig. 8. SEM micrograph of cross sectional view of the glassy coating.

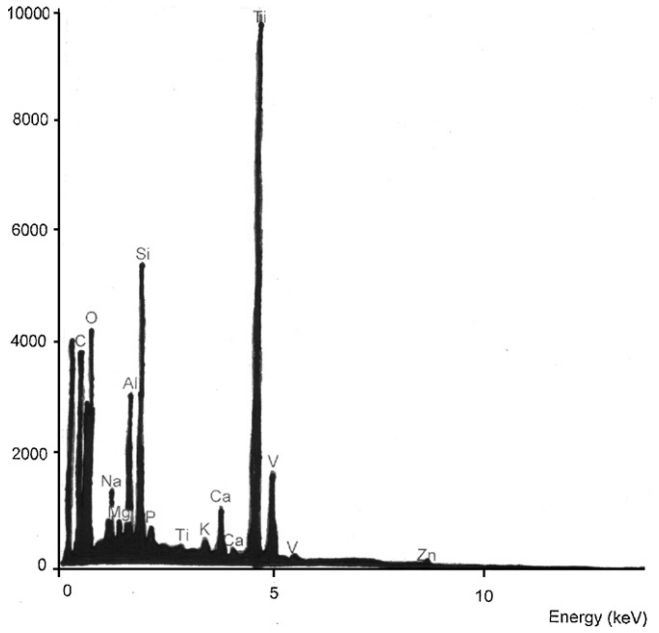


Fig. 9. EDX pattern of the interface area in the micrograph.

coatings, respectively). However, it was observed that addition of more than 10 wt% of nano-HAp powder did not improve the adhesion strength any more. This supports the findings of our earlier reported results [18].

When seen under image analyzer, fine cracks (originating from the indentation site and moving across the glassy coating away in all direction) were found to be present in case of Figs. 11 and 13, a characteristic feature of brittle glass coating; where as they were almost absent in composite coatings (Figs. 12 and 14). The glassy coatings fractured out as flakes as the normal load was increased. In case of composite coatings, the scratch patterns were more or less smooth with regular material removal along the scratch path because of its more glass ceramic characteristics. Some small cracks were observed in the scratch path, which moved perpendicular to scratch direction failing to penetrate the composite matrix.

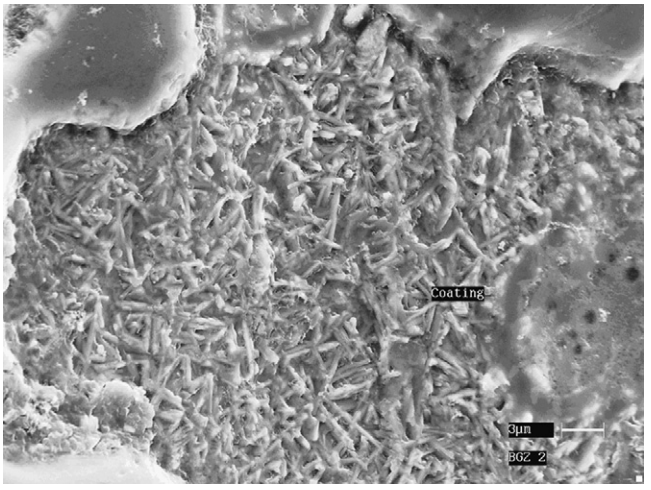


Fig. 10. Magnified view of bioactive glass coating.

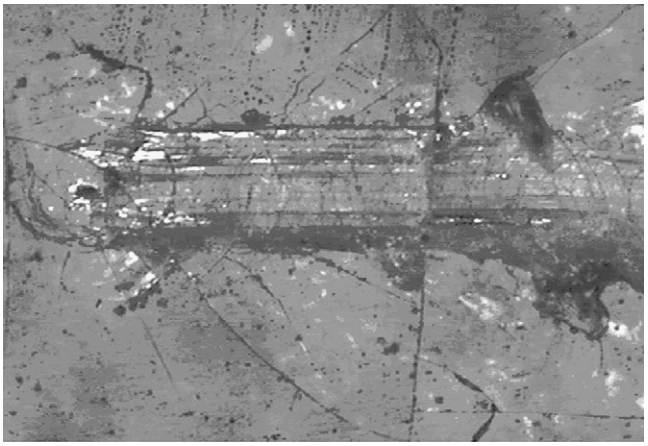

Fig. 11. A typical optical micrograph of scratch tested bioglass surface (BGZ-1).

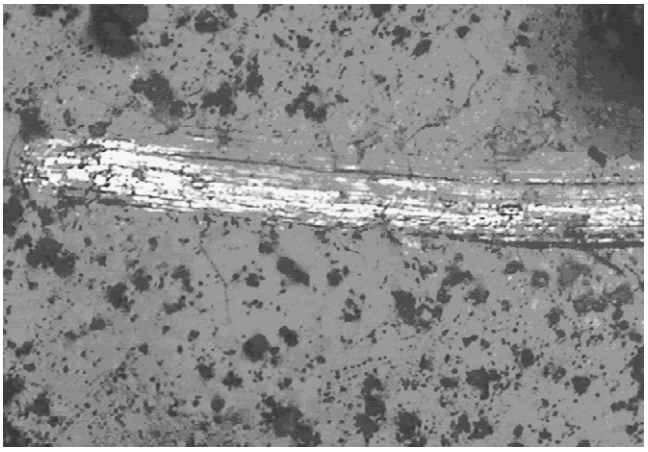

Fig. 14. A typical optical micrograph of scratch tested bioglass nano HAp (10 wt%) composite coating surface (BGZ-2).

### 3.1.6. Pull off adhesion strength analysis of coatings

Pull off adhesion strength of the coatings was measured in order to estimate the adhesion strength of the coatings. The results showed in Table 4 clearly indicate that different glasses behave in different manner as seen in case of scratch testing measurements. In case of BGZ-1 the addition of nano-HAp increases the adhesion strength up to 25% addition but in case of BGZ-2 the trend is reversed, where addition of nano-HAp reduces the adhesion strength.

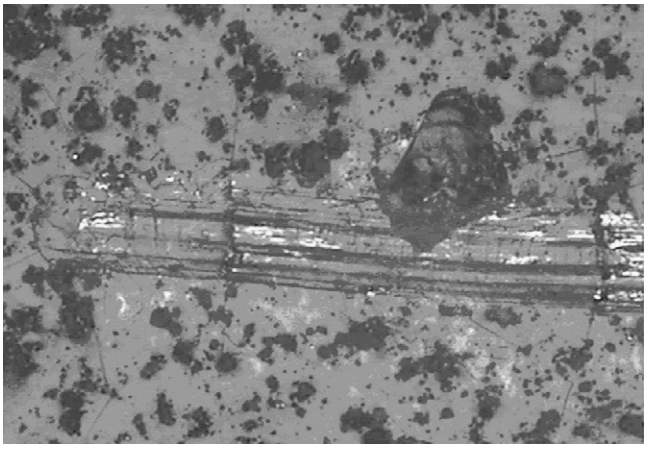

Fig. 12. A typical optical micrograph of scratch tested bioglass nano HAp (10 wt%) composite coating surface (BGZ-1).

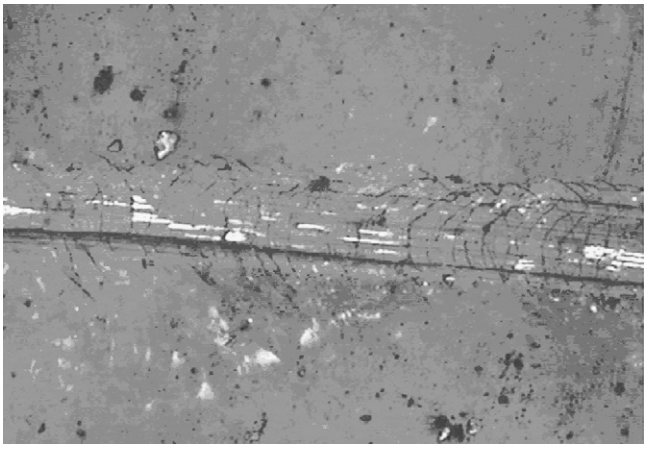

Fig. 13. A typical optical micrograph of scratch tested bioglass surface (BGZ-2).

## 3.2. In vitro analysis of coatings

### 3.2.1. Cytotoxicity test

In vitro cytotoxicity test was performed on BGZ-1 and BGZ-2 coated samples, corresponding porous and dense scaffolds and the glass powders as such. Both direct contact and tests on extracts were performed as per ISO 10993-5, 1999 standard specification. Cellular responses were scored as non-cytotoxic, mildly cytotoxic, moderately cytotoxic and severely cytotoxic. Negative control gave non-cytotoxic response and positive control gave severely cytotoxic response as expected. The test reports of all the bioactive glasses indicate that all the materials tested are non-cytotoxic in both the direct and test on extract methods as shown in Figs. 15 and 16.

Table 3
Effect of nano HAp addition on breaking strength by scratch testing of different composite coating.

| Bioactive glass | % of nano HAp addition | | |
|---|---|---|---|
| | 0 | 10 | 25 |
| BGZ-1 | 21 | 26.5 | 26 |
| BGZ-2 | 41.5 | 42.5 | 33 |

Table 4
Effect of nano HAp addition on pull off adhesion strength of different bioglass and composite coatings on Ti–6Al–4V substrate.

| Serial no. | Coating composition | Average adhesion strength (MPa) |
|---|---|---|
| 1. | BGZ-1 | 5.63 |
| 2. | BGZ-2 | 17.54 |
| 3. | BGZ-1 + 10% HAp | 10.09 |
| 4. | BGZ-2 + 10% HAp | 12.00 |
| 5. | BGZ-1 + 25% HAp | 16.71 |
| 6. | BGZ-2 + 25% HAp | 4.57 |

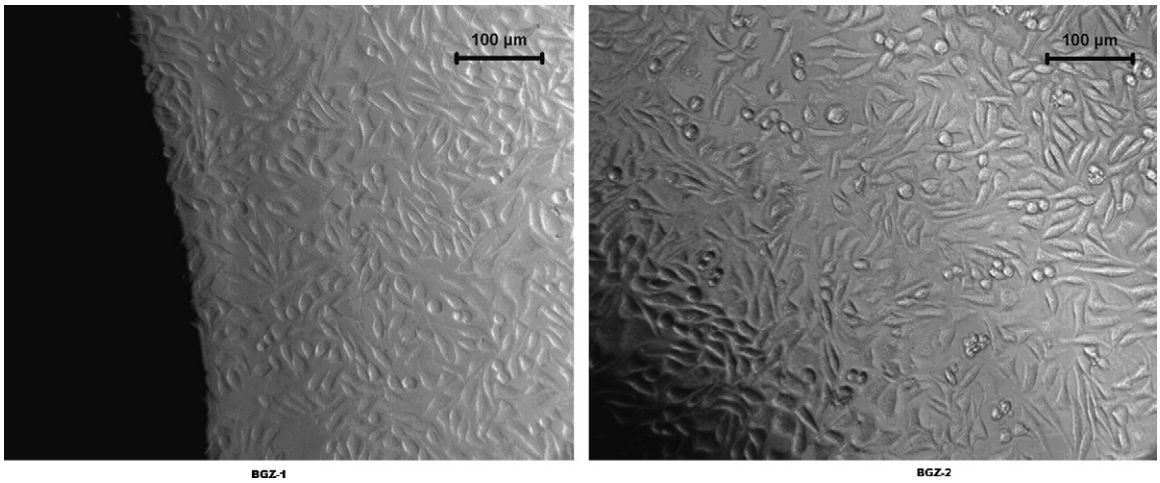


Fig. 15. Phase contrast micrograph of cells in direct contact with BGZ glass coating.

BGZ glasses did not show any signs of toxicity after 24 h with L929 cells (Figs. 15 and 16). The cells appeared spindle in shape and formed a monolayer. The cytotoxic scale was measured as zero, which corresponds to non-cytotoxicity. Phase contrast micrograph of porous and dense scaffolds and the glass powders showed similar micrographs under identical test conditions which is normally expected, because the cytotoxicity depends on material characteristics and in these cases the material is same for every sample which only differ in processing conditions. The results indicated that the zinc containing bioglass, their composites with nano-sized HAp, their coating on Ti–6Al–4V substrate and the dense or porous scaffolds are all highly biocompatible materials and could potentially serve as an effective material for in vivo applications [37,38].

### 3.2.2. Dissolution study of bioactive glass blocks

In order to understand the biological behaviour (acellular bioactivity) of these bioactive glass materials inside the living system, dissolution study in simulated body fluid was carried out. Many variables are known to influence the dissolution and subsequent mechanisms that lead to carbonated hydroxyapatite layer formation and bioactivity of glasses [39–42]. The solutions after dissolution study of different bio-glasses in different medium were collected at definite time intervals and chemically analysed by ICP. Composition of zinc in bioactive glass is very low and hence its release is expected to be in trace quantities. In order to avoid errors in analysis of zinc due to the presence of other alkalis in SBF, distilled water was selected as the medium. The results were plotted in Figs. 17 and 18. The $Ca^{2+}$ as well as $PO_4^{3-}$ ion concentrations released with increasing time is shown in Fig. 17. The concentration of silicon ion in surrounding medium remains very low and constant throughout the study period. In the initial period of two weeks, different glasses behave in a different manner. In case of BGZ-1 the concentration of ions decreases slowly and between 2 and 3 weeks concentration is very less compared to 3–4 week. In case of BGZ-2, in first two weeks concentration of $Ca^{2+}$ increases, followed by decrease in 2–3 week and again increases in 3–4 week. It was observed that during dissolution fine crystals of Hap deposits as a colony on the corroded spots of the immersed surface. The surrounding glass surface is either

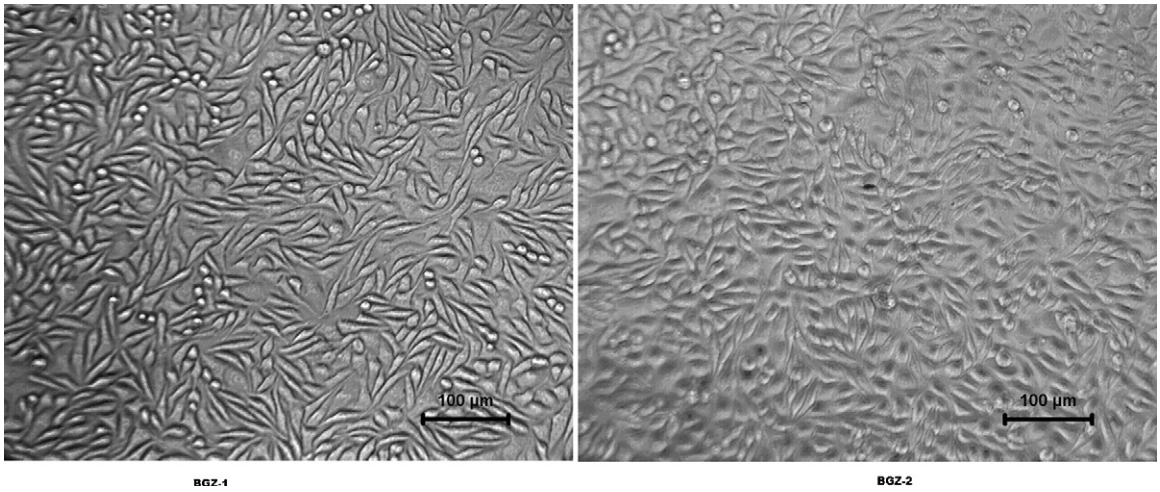


Fig. 16. Cellular response after cytotoxicity test on bio-glass coating by direct contact method.

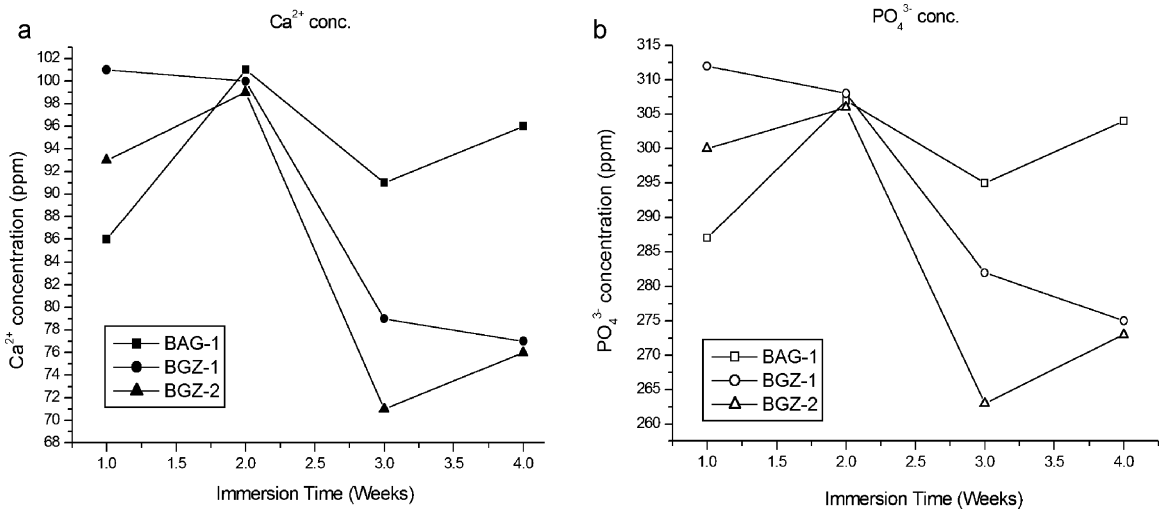


Fig. 17. (a) $Ca^{2+}$ and (b) $PO_4^{3-}$ ion concentrations of different glasses after immersion in SBF up to 4 weeks.

free or scarcely deposited with precipitated Hap crystals [43]. This observation again proves the theory that Hap crystals are deposited due to some biochemical reactions occurring at the corroded surface of the bioactive glass (exposed Si–OH network) during dissolution in simulated body fluid and the results differ with different bioactive glasses depending upon the bioactivity [25]. In fact, after exposure to SBF solution the alkali and alkaline earth ions from the bioactive glass surface start diffusing into the surrounding medium, leaving behind a corroded surface with increasing surface area and thus increasing rate of dissolution. Further, leaching of ions leads to an exposition of Si–OH networked surface. This active surface stimulates deposition of Calcium hydroxyapatite fine crystals on the bioactive glass surface which slowly reduces the area of exposed surface and as a result the decrease in rate of dissolution. The nature of deposited particles are different, in BGZ-1 the grains are cubic and regular whereas, in BGZ-2, the deposited Hap particles are elongated nodular in shape (Figs. 19 and 20). EDX analysis showed both the grains as pure calcium phosphate phase. Further, an increase in $Ca^{2+}$ as well as $PO_4^{3-}$ ion concentrations occurred up to 2 weeks of immersion for all the glasses except BGZ (where it remains almost unchanged) which implies a leaching out of these ions from the glass blocks but no simultaneous removal of these ions through precipitation of HAp crystals. However, after or around 2 weeks, precipitation of Ca–P phase (HAp) occurred which results in decrease in concentration of these ions in the solution. The precipitated HAp phase can be confirmed from the chemical analysis results and the SEM micrographs studied in regular intervals.

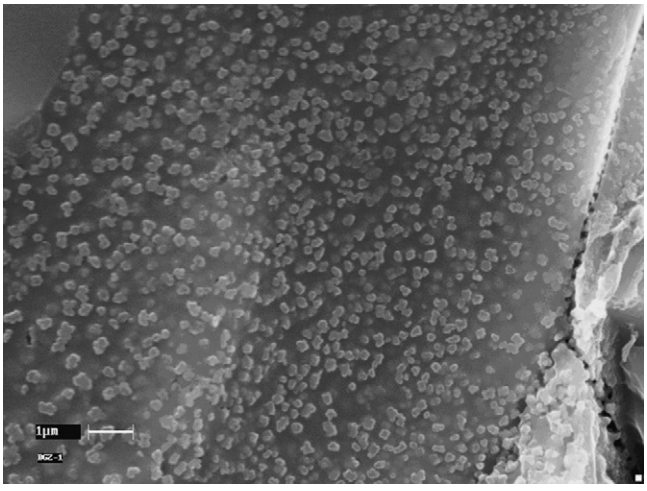


Fig. 18. Micrograph after two weeks dissolution of BGZ-1 coating.

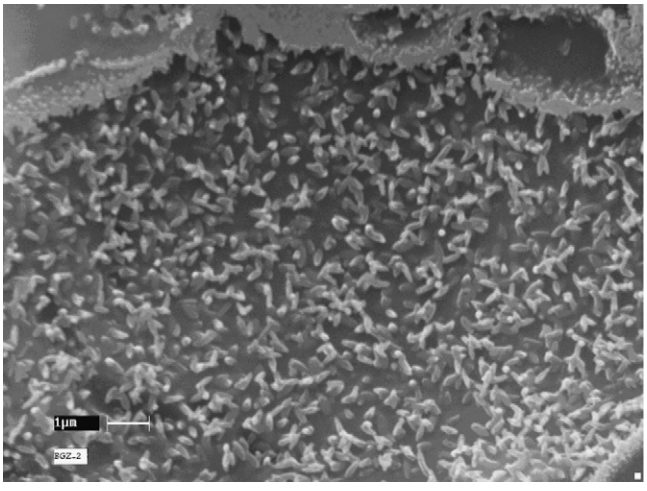


Fig. 19. Micrograph of BGZ-2 coating after dissolution in SBF.

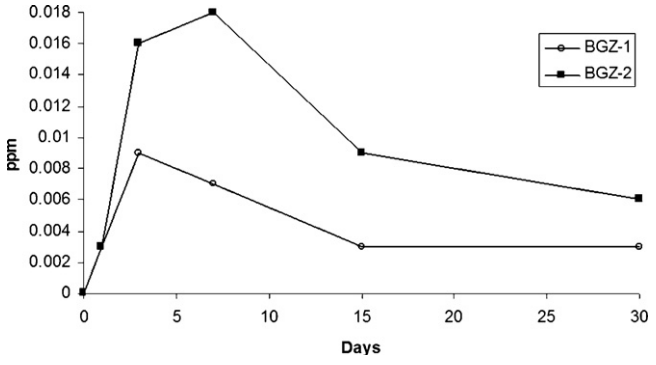


Fig. 20. Zinc release rate in distilled water.

Release of $Zn^{++}$ ions in distilled water follows a different trend, increases with time reaching maxima and then decreases almost asymptotically (Fig. 18). The amount of $Zn^{++}$ released increases with zinc content in the glass. However, the released $Zn^{++}$ concentration is very much within the toxicity limit in human body.

## 4. Conclusion

The novel zinc containing bioactive glass compositions developed and reported in this paper can be prepared by conventional glass melting technique and further processed to yield porous or dense scaffolds and bone filler materials by simple ceramic processing techniques. The bioactive glass and their composite coating (with nanosized HAp) on Ti–6Al–4V alloy can be prepared by simple vitreous enamelling method.

These glasses are thermally stable and do not change their structure and properties with rate of heating. The composite coating exhibits significantly improved scratch resistance property, which are expected to resist the surface degradation due to friction with the surrounding hard tissues during initial insertion of the coated load bearing implants. This property can also improve the performance of the coated implants in achieving better primary strength during cementless fixation. The cytotoxic evaluation shows that these glasses are non cytotoxic and after processing into scaffolds or coatings their biological response remain unaltered making them suitable for in vivo applications. The dissolution behaviour of these glasses in simulated body fluid and distilled water showed them to be biologically active over a couple of weeks period with simultaneous dissolution of calcium and phosphate ions (over a period of weeks) resulting in precipitation of carbonated hydroxyapatite microcrystals on the surface. This step is essential for effective Osseo integration of the biomaterial with the surrounding hard tissues. Simultaneous release of zinc ions in a controlled fashion over a time period of 3–4 weeks observed in this study may also help further osseous growth. However, the mechanism of deposition of precipitated HAp with different microstructure for different bioactive glass surface is not clear. Further in vivo and animal study is essential to establish its bioactivity in actual living system.

## Conflicts of interest

None.

## Acknowledgements

The authors wish to thank The Director, CG&CRI for his kind interest in this work. All the personnel related to the characterization of the materials are sincerely acknowledged.

## References

[1] S.D. Cook, K.A. Thomas, J.F. Kay, M. Jarcho, Hydroxyapatite coated porous titanium for use as an orthopedic biologic attachment system, Clin. Orthop. Relat. Res. 230 (1988) 303–312.
[2] C. Soundrapandian, S. Datta, B. Sa, Drug eluting implants for osteomyelitis, Crit. Rev. Ther. Drug Carrier Syst. 24 (2007) 493–545.
[3] A. Pazo, E. Saiz, A.P. Tomsia, Silicate glass coatings on Ti-based implants, Acta Mater. 46 (1998) 2551–2558.
[4] J.M. Gomez-Vega, E. Saiz, A.P. Tomsia, Glass-based coatings for titanium implant alloys, J. Biomed. Mater. Res. 46 (1999) 549–559.
[5] C. Soundrapandian, B. Sa, S. Datta, Organic–inorganic composites for bone drug delivery, AAPS Pharm. Sci. Technol. 10 (2009) 1158–1171.
[6] A. Ito, K. Ojima, H. Naito, N. Ichinose, T. Tateishi, Preparation, solubility, and cytocompatibility of zinc-releasing calcium phosphate ceramics, J. Biomed. Mater. Res. 50 (2000) 178–183.
[7] A. Ito, H. Kawamura, M. Otsuka, M. Ikeuchi, H. Ohgushi, K. Ishikawa, K. Onuma, N. Kanzaki, Y. Sogo, N. Ichinose, Zinc-releasing calcium phosphate for stimulating bone formation, Mater. Sci. Eng. C 22 (2002) 21–25.
[8] M. Yamaguchi, R. Yamaguchi, Action of zinc on bone metabolism in rats increases in alkaline phosphatase activity and DNA content, Biochem. Pharmacol. 35 (1986) 773–777.
[9] D.B. Jaroch, D.C. Clupper, Modulation of zinc release from bioactive sol–gel derived $SiO_2$–CaO–ZnO glasses and ceramics, J. Biomed. Mater. Res. A 82 (2007) 575–588.
[10] V. Salih, A. Patel, J.C. Knowles, Zinc-containing phosphate-based glasses for tissue engineering, Biomed. Mater. 2 (2007) 11–20.
[11] S. Kanno, C.D. Anuradha, S. Hirano, Localization of zinc after in vitro mineralization in osteoblastic cells, Biol. Trace Elem. Res. 83 (2001) 39–47.
[12] S. Kanno, C.D. Anuradha, S. Hirano, Chemotactic responses of osteoblastic MC3T3-E1 cells toward zinc chloride, Biol. Trace Elem. Res. 83 (2001) 49–55.
[13] K.J.M. Söderholm, E. Mondragon, I. Garcea, Use of zinc phosphate cement as a luting agent for DenzirTM copings: an in vitro study, BMC Oral Health 3 (2003) 1–8.
[14] L. Linati, G. Lusvardi, G. Malavasi, L. Menabue, M.C. Menziani, P. Mustarelli, U. Segre, Qualitative and quantitative structure–property relationships (QSPR) analysis of multicomponent potential bioactive glasses, J. Phys. Chem. B 109 (2005) 4989–4998.
[15] G. Lusvardi, G. Malavasi, L. Menabue, M.C. Menziani, A. Pedone, U. Segre, A computational tool for the prediction of crystalline phases obtained from controlled crystallization of glasses, J. Phys. Chem. B 109 (2005) 21586–21592.
[16] A. Oki, B. Parveen, S. Hossain, S. Adeniji, H. Donahue, Preparation and in vitro bioactivity of zinc containing sol–gel-derived bioactive glass materials, J. Biomed. Mater. Res. A 69 (2004) 216–221.
[17] T. Kokubo, H. Kushitani, S. Sakka, T. Kitsugi, T. Yamamuro, Solutions able to reproduce in vivo surface-structure changes in bioactive glass–ceramic, J. Biomed. Mater. Res. 24 (1990) 721–734.
[18] S. Bharati, C. Soundrapandian, S. Datta, D. Basu, Bioglass coating on Ti-alloy: effect of second phase and γ-irradiation on mechanical property, J. Eur. Ceram. Soc. 29 (2009) 2527–2535.
[19] S.K. Ghosh, S.K. Nandi, B. Kundu, S. Datta, D.K. De, S.K. Roy, D. Basu, Interfacial response of hydroxyapatite and tri-calcium phosphate prepared by a novel aqueous combustion method: a comparison with bioglass *in vivo* implanted in goat, J. Biomed. Mater. Res. B 86 (2008) 217–227.
[20] S.K. Nandi, B. Kundu, S. Datta, D.K. De, D. Basu, The repair of segmental bone defects with porous bioglass: an experimental study in goat, Res. Vet. Sci. 86 (2009) 162–173.
[21] S.K. Nandi, B. Kundu, P. Mukherjee, T.K. Mandal, S. Datta, D.K. De, D. Basu, In vitro and in vivo release of cefuroxime axetil from bioactive glass as an implantable delivery system in experimental osteomyelitis, Ceram. Int. 35 (2009) 3207–3216.
[22] T. Kokubo, H. Kushitani, S. Sakka, T. Kitsugi, T. Yamamuro, Solutions able to reproduce in vivo surface-structure changes in bioactive glass–ceramic A-W, J. Biomed. Mater. Res. 24 (1990) 721–734.
[23] S. Mistry, D. Kundu, S. Datta, D. Basu, Effects of bioactive glass, hydroxyapatite and bioactive glass–hydroxyapatite composite graft particles in the treatment of periapical defects, Clin. Dent. J. 4 (2010) 53–59.
[24] S.K. Ghosh, A. Prakash, S. Datta, S.K. Roy, D. Basu, Effect of fuel characteristics on synthesis of calcium hydroxyapatite by solution combustion route, Bull. Mater. Sci. 33 (1) (2010) 7–16.
[25] L.L. Hench, Bioceramics: from concept to clinic, J. Am. Ceram. Soc. 74 (1991) 1487–1510.

[26] B.R. Lawn, A.G. Evans, D.B. Marshall, Elastic/plastic indentation damage in ceramics: the median/radial crack system, J. Am. Ceram. Soc. 63 (1980) 574–581.
[27] D.R. Dukino, M.V. Swain, Comparative measurement of fracture toughness with berkovich and vickers indenters, J. Am. Ceram. Soc. 75 (1992) 3299–3304.
[28] J. Chen, S.J. Bull, Assessment of the toughness of thin coatings using nanoindentation under displacement control, Thin Solid Films 494 (2006) 1–7.
[29] L.P. Mullins, M.S. Bruzzi, P.E. McHugh, Measurement of the microstructural fracture toughness of cortical bone using indentation fracture, J. Biomech. 40 (2007) 3285–3288.
[30] S. Agathopoulos, D.U. Tulyaganov, J.M.G. Ventura, S. Kannan, M.A. Karakassides, J.M.F. Ferriera, Formation of hydroxyapatite onto glasses of the CaO–MgO–$SiO_2$ system with $B_2O_3$, $Na_2O$, $CaF_2$ and $P_2O_5$ additives, Biomaterials 27 (2006) 1832–1840.
[31] J.M. Gomez-Vega, E. Saiz, A.P. Tomsia, G.W. Marshall, S.W. Marshall, Bioactive glass coatings with hydroxyapatite and bioglass particles on Ti-based implants. 1. Processing, Biomaterials 21 (2000) 105–111.
[32] D.C. Clupper, L.L. Hench, Crystallization kinetics of tape cast bioactive glass 45S5, J. Non-Cryst. Solids 318 (2003) 43–48.
[33] I.W. Donald, Preparation, properties and chemistry of glass- and glass–ceramic-to-metal seal and coatings, J. Mater. Sci. 28 (1993) 2841–2886.
[34] S.J Bull, E.G. Berasetegui, An overview of the potential of quantitative coating adhesion measurement by scratch testing, Tribol. Int. 39 (2006) 99–104.
[35] J. Forsgren, F. Svahn, T. Jarmar, H. Engqvist, Formation and adhesion of biomimetic hydroxyapatite deposited on titanium substrates, Acta Biomater. 3 (2007) 980–984.
[36] J. Valli, A review of adhesion test methods for thin hard coatings, J. Vac. Sci. Technol. A4 (1986) 3001–3014.
[37] T.-C. Kuo, B.-S. Lee, S.-H. Kang, F.-H. Lin, C.-P. Lin, Cytotoxicity of DP-bioglass paste used for treatment of dentin hypersensitivity, J. Endod. 33 (2007) 51–454.
[38] K. Zhang, N.R. Washburn, C.G. Simon Jr., Cytotoxicity of three-dimensionally ordered macroporous sol–gel bioactive glass (3DOM-BG), Biomaterials 26 (2005) 4532–4539.
[39] P. Sepulveda, J.R. Jones, L.L. Hench, In vitro dissolution of melt-derived 45S5 and sol–gel derived 58S bioactive glasses, J. Biomed. Mater. Res. A 61 (2002) 301–311.
[40] J.R. Jones, P. Sepulveda, L.L. Hench, Dose-dependent behavior of bioactive glass dissolution, J. Biomed. Mater. Res. B 58 (2001) 720–726.
[41] J.R. Jones, L.M. Ehrenfried, P. Saravanapavan, L.L. Hench, Controlling ion release from bioactive glass foam scaffolds with antibacterial properties, J. Mater. Sci.: Mater. Med. 17 (2006) 989–996.
[42] H. Ylänen, K.H. Karlsson, A. Itälä, H.T. Aro, Effect of immersion in SBF on porous bioactive bodies made by sintering bioactive glass microspheres, J. Non-Cryst. Solid 275 (2000) 107–115.
[43] G. Bolelli, V. Cannillo, R. Gadowb, A. Killinger, L. Lusvarghi, J. Rauch, Microstructural and in vitro characterisation of high-velocity suspension flame sprayed (HVSFS) bioactive glass coatings, J. Eur. Ceram. Soc. 29 (2009) 2249–2257.